ACS Sustainable Chemistry & Engineering

Research Article

pubs.acs.org/journal/ascecg

Single-Step, Plasma-Enabled Reforming of Natural Precursors into Vertical Graphene Electrodes with High Areal Capacitance

Dong Han Seo,[†,‡] Samuel Yick,[†,‡] Shafique Pineda,[†,‡] Dawei Su,[§] Guoxiu Wang,[§] Zhao Jun Han,[†] and Kostya (Ken) Ostrikov*[,†,‡,∥]

[†]Plasma Nanoscience, Industrial Innovation Program, CSIRO Manufacturing Flagship, Lindfield, New South Wales 2070, Australia

[‡]School of Physics, The University of Sydney, Sydney, New South Wales 2006, Australia

[§]School of Chemistry and Forensic Science, University of Technology Sydney, Sydney, New South Wales 2007, Australia

[∥]School of Chemistry, Physics and Mechanical Engineering, Queensland University of Technology, Brisbane, Queensland 4000, Australia

S *Supporting Information*

ABSTRACT: Graphene nanostructures possess excellent physical properties such as high surface area, good mechanical stability, and good electric conductivity, which make them attractive as electrodes for high-performance energy storage devices. However, graphene-based nanomaterials have yet to be materialized into commercial energy storage devices, mainly due to the high cost in fabrication processes and the difficulty in achieving high mass loading. In particular, the high mass loading of active materials on the electrode represents an important step toward the translation of excellent electrochemical activity seen in the microscopic regime into the practical applications. Here, supercapacitor electrodes made of vertical graphene nanosheets (VGNS) are fabricated from a range of commercially available cheese precursors via green, low-temperature, plasma-based reforming processes. Taking advantage of the fast solidification of cheese molecules and plasma−matter interactions, the produced VGNS exhibit a high mass loading of 3.2 mg/cm^2 and a high areal capacitance of 0.46 F/cm^2. These results demonstrate a single-step, scalable, environmentally benign, and cost-effective approach for the transformation of natural precursors into high-quality graphene structures, which could be promising for a variety of advanced electronic and energy applications.

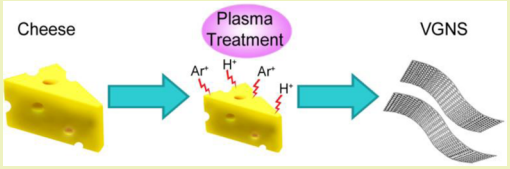

KEYWORDS: *Vertical graphene nanosheets, Supercapacitor, Natural precursor, High mass loading, High areal capacitance*

INTRODUCTION

Research in electrochemical energy storage has recently seen a drastic expansion due to the increasing energy demands for portable electronics, electric vehicles, and utilization of renewable energy resources.[1−4] Of the various energy storage devices, supercapacitors represent a particularly attractive option, as they offer high power density, rapid charge/discharge, and a long lifespan, which are critical for a number of energy storage applications.[5,6] Fundamentally, supercapacitors operate by storing ions within the electric double layer (EDL) or through redox reactions on the electrode surface.[7] Such mechanisms allow supercapacitors to have better cycling performance and power density as compared to other energy storage devices such as batteries.[6] Nevertheless, the widespread applications of current supercapacitors are impeded by their low energy density.

The physical properties of electrode materials are known to dictate the performance of supercapacitors. In general, a large surface area with easily accessible sites and high electrical conductivity is required for an electrode to deliver high energy and power densities. The advent of carbon nanostructures such as carbon nanotubes and graphene has introduced materials with intrinsically high surface area and excellent electrical conductivity, which are highly promising for energy storage applications.[8,9] A good example is vertical graphene nanosheets (VGNS), which recently emerged as a promising electrode material owing to its highly favorable structural and electrochemical properties.[10,11] VGNS possess a unique morphology of few-layered graphene sheets self-organized in an open, interconnected, and three-dimensional (3D) array structure. While the open structure of VGNS can facilitate the rapid formation of EDL, its structural rigidity enhances stability by preventing the restacking of graphene nanosheets, a commonly observed problem in horizontal graphenes when immersed in liquid electrolytes.[12−14] Supercapacitor electrodes made of VGNS have shown many notable charge storage features, such as high specific capacitance, stable charge retention capability, and a low relaxation time constant τ_0.[10,15]

However, the biggest challenge of implementing VGNS into practical supercapacitors is the low mass loading. VGNS grown by chemical vapor deposition (CVD) usually have a mass loading of <0.5 mg/cm^2 (thickness <4 μm).[16] As such, the high specific capacitance (C_s) of the materials does not always lead to a high areal capacitance (a more accurate measure for the

Received: December 14, 2014
Revised: January 22, 2015
Published: February 12, 2015

DOI: 10.1021/sc500806s
ACS Sustainable Chem. Eng. 2015, 3, 544−551

practical supercapacitor devices) due to the limited quantity of active materials present on the electrodes.[17] This problem cannot be mitigated by long growth time, as it often results in the formation of undesired amorphous carbons rather than a thicker VGNS structure. On the other hand, a few chemical-based methods have recently reported a high mass loading of graphene-based materials.[18] However, in these chemical-based syntheses, the extraction of graphene-based materials from natural graphite precursors is not only precursor-specific but also expensive and complicated, as well as energy, time, and resource demanding. Moreover, these processes usually require additional materials, such as binders or gels, to integrate these nanostructures into functional electrodes, further complicating the process of device fabrication and reducing the scalability and sustainability.[19−23] Therefore, there is a need for developing a simple and green process that can directly produce high-quality VGNS at high mass loading for supercapacitor applications.

In our previous work, we have demonstrated the versatility and effectiveness of plasmas as a simple and green nanofabrication tool for the efficient transformation of natural precursors into VGNS electrodes.[24−26] Notably, by utilizing precursors such as butter, this enabled the growth of VGNS with a high C_s of about 200 F/g and excellent stability of more than 8000 cycles. However, the areal capacitance (C_A) of these electrodes remained unsatisfactory due to limited mass loading. In this work, we solve this problem by employing cheese as the natural precursor in the plasma-based fabrication process. We demonstrate a single-step, plasma-based reforming process to produce VGNS electrodes with a high mass loading up to 3.2 mg/cm^2 and excellent areal capacitance, which are superior compared to other graphene-based materials obtained by the conventional fabrication techniques such as chemical or thermal processing. Our results thus represent significant progress toward translating the excellent capabilities of graphenes into functional high-performance energy storage devices.

EXPERIMENTAL SECTION

Fabrication of VGNS from Cheese Precursors. The single-step, plasma-enabled transformation of cheese precursors into VGNS was carried out in a RF inductively coupled plasma CVD system. Commercially available processed cheese, cream cheese, and fat-free processed cheese were used as precursors. In order to provide a uniform coating on the Ni foam substrates, the cheese precursors were first melted at 80 °C. This allowed the substrates to be evenly coated with the liquefied cheese. The cheese−laden substrates were then removed from the heater so that the cheese could resolidify prior to loading in the plasma reactor. A gas mixture of 5 sccm Ar and 20 sccm H_2 was then fed into the reactor, where the plasma was ignited at a pressure and RF power of 2.0 Pa and 1000 W, respectively. Although no external substrate heating was used, during the 10 min plasma process, the substrate temperature reached approximately 400 °C due to the plasma-heating effects. To reduce the amount of amorphous carbon formed in the growth process, the as-grown samples were treated in air at 300 °C for 1 h.

Material Characterization. Field-emission scanning electron microscopy (FE-SEM) images were obtained by a Zeiss Auriga microscope operated at 5 keV electron beam energy with an InLens secondary electron detector. Raman spectroscopy was performed using a Renishaw inVia spectrometer with laser excitation at 514 nm (Ar laser) and a probing spot size of about 1 μm^2. X-ray photoelectron spectroscopy (XPS) spectra were recorded by a Specs SAGE 150 spectroscope with Mg Kα excitation at 1253.6 eV. Both survey and narrow scans were conducted. The mass of the electrode was determined by weighing a 10 cm long sample on a ultrasensitive balance ($\Delta \pm 0.1$ μg; Mettler Toledo UMT2) and calculating the fractional mass submerged into the electrolyte. N_2 adsorption−desorption isotherms of VGNS were measured by using a Micromeritics 3Flex analyzer at the temperature of 77 K. Brunauer−Emmett−Teller (BET) analysis was used to determine the surface area and was calculated using the isothermal points at a relative pressure of $P/P_0 = 0.05−0.25$.

Electrochemical Measurements. The electrochemical measurements were performed in 1 M Na_2SO_4 electrolyte. Both three- and two-electrode cell configurations were employed. The three-electrode cell used the VGNS sample as the working electrode, Pt foil as the counter electrode, and Ag/AgCl reference electrode; while the two-electrode cell used two identical VGNS samples as the electrodes. Cyclic voltammetry (CV), galvanostatic charge/discharge, and electrochemical impedance spectroscopy (EIS) measurements were conducted using a BioLogic VSP 300 potentiostat/galvanostat device. CV tests were performed in the potential range of 0−0.8 V at scan rates of 5−100 mV s^{-1}. Galvanostatic charge/discharge curves were obtained at current densities of 6, 5, and 4 mA/cm^2 for VGNS derived from processed cheese and 3, 2, and 1 mA/cm^2 for VGNS derived from cream cheese. EIS measurements were performed in the frequency range from 0.01 Hz to 100 kHz. The specific capacitance of the single electrode, C_s, was calculated from the CV curves of two-electrode measurements by integrating the discharge current against the potential, V, according to $C_s = 2\int[\mathrm{I\ dV}]/\nu m\Delta V$, where ν is the scan rate (V s^{-1}), m is the mass of the active material in a single electrode, and ΔV is the operating potential window (0.8 V). The mass loading was 3.2, 0.8, and 2.8 mg/cm^2 for VGNS derived from processed cheese, cream cheese, and fat-reduced cheese, respectively. Similarly, C_s was calculated from the CV curves of three-electrode measurements by the equation $C_s = \int[\mathrm{I\ dV}]/\nu m\Delta V$.

RESULTS AND DISCUSSION

Figure 1 shows the schematic of the single-step, plasma-enabled reforming of cheese into VGNS. Ni foam was chosen as the

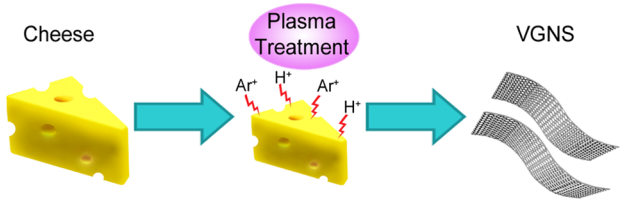

Figure 1. Schematics of the experimental process that transforms the cheese precursor into vertical graphene nanosheets (VGNS).

substrate for VGNS as it provides a porous 3D scaffold for the growth of VGNS. Furthermore, due to its good electrical conductivity, Ni foam also functions as the current collector. The VGNS were grown from the cheese precursors by a 10 min exposure to plasmas in an argon and hydrogen gas mixture to enable the growth of VGNS. Commercially available processed cheese was used as the carbon source. Processed cheese is made via blending natural cheese of different age and maturity.[27] As the production of processed cheese is a standardized industrial process, this will ensure that variation between different cheese cultures, which might affect the experimental reproducibility, can be minimized.

Processed cheese consists of fats, proteins (mostly casein), and water in 30, 22, and 40 wt %, respectively.[27,28] In contrast, cream cheese possesses a significantly higher water content, and the fat, protein and water content of cream cheese are 30, 10, and 55 wt %, respectively.[29] In both cheeses, there exist a small quantity of salt, emulsifying agents, and other addictives. During the early growth process, the cheese precursor was

DOI: 10.1021/sc500806s
ACS Sustainable Chem. Eng. 2015, 3, 544−551

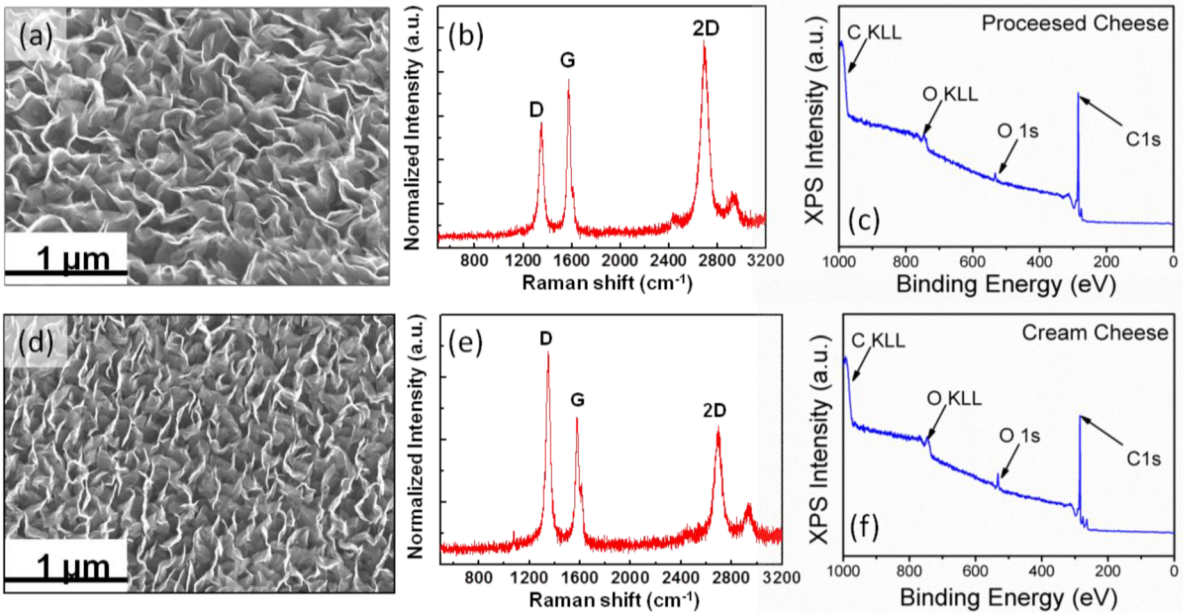

Figure 2. Typical SEM images of VGNS produced from processed cheese (a) and cream cheese (d) precursors. Raman spectra of the VGNS obtained from processed cheese (b) and cream cheese (e). (c,f) XPS spectra of both cheese precursors showed that the resulting nanostructures were composed of carbon with a trace amount of oxygen.

promptly dehydrated by the low pressure environment and plasma heating effects. Subsequently, the heterogeneous carbon precursors (i.e., fat and protein groups) were broken down into simple hydrocarbon building units by the rapid plasma dissociation of the material. These building units then self-organized into VGNS on the plasma-exposed surfaces. Such plasma-specific effects can be attributed to the strong plasma–matter interactions in the plasma sheath. The plasma process made it possible to achieve a high mass loading of VGNS, which could also be extracted as high-quality graphene powder (Figure S1a–c, Supporting Information). The typical SEM image also confirmed VGNS with total coverage on the nickel foam substrate (Figure S1d, Supporting Information).

Owing to the above-mentioned advantages, VGNS produced with the two cheese precursors, i.e., processed and cream cheeses, showed mass loadings of 3.2 and 0.8 mg/cm^2, respectively, which are higher than what is normally obtained from gaseous or other solid state precursors in a similar plasma process.[24−26] Previously, we have demonstrated the growth of VGNS from gaseous, liquid, and solid state natural precursors. In these experiments, we noticed that the growth of VGNS from liquid precursors enabled a strong adhesion to the substrate and minimized the undesired formation of amorphous carbon. These properties are highly attractive for the integration of VGNS in supercapacitor electrodes.[26] However, due to their fluidic nature, liquid-based precursors may lead to a significant loss of precursor material during the growth process. The loss may result from the initial growth stage when the precursor was undergoing a transformation from the liquid (precursor) to the solid state (VGNS), as well as from the plasma dissociation and etching stage. Consequently, this leads to poor efficiency of VGNS growth with a relatively low mass loading. Therefore, to fabricate an electrode with a high mass loading while maintaining the favorable properties as exhibited from liquid-based precursors, we searched for a semi-liquid precursor that can rapidly solidify upon losing its water content. A strong intermolecular bonding in the precursor was also desired as this could minimize the possible loss of precursor material during the plasma reforming process. To meet these requirements, cheese represents a particularly promising candidate for the improved efficiency of reforming natural precursors into functional VGNS structures with high mass loading. Indeed, as cheese can quickly transform into the solid state after losing its water content, its unique intermolecular structure can minimize possible loss of material during the transformation process.

Panels (a) and (d) of Figure 2 show the high-resolution SEM images of VGNS derived from processed and cream cheeses, respectively. These images show a uniform, dense, 3-D network of thin graphene nanosheets. Such uniform transformation demonstrates the merits of plasma as a nanofabrication tool to build functional nanostructures from heterogeneous natural precursors.[25] Panels (b) and (e) of Figure 2 show the Raman spectra of VGNS derived from processed and cream cheeses, respectively. The Raman spectra reveal the high graphitic content of the VGNS. For both the processed and cream cheeses, three distinct Raman peaks were present, namely, the characteristic disorder peak (D-band) arising from the defects within the sp^2 carbon materials at 1350 cm^{-1}, graphitic peak (G-band) from the in-plane vibrational E_{2g} mode of the graphitic lattice at 1579 cm^{-1}, and second-order 2D-band due to the three-dimensional interplanar stacking of hexagonal carbon networks at 2700 cm^{-1}.[30−33] By examining the ratios of intensities between the peaks, the quality of VGNS can be determined. Specifically, the I_D/I_G ratio reflects the degree of defects present within the graphene lattice, whereas the I_{2D}/I_G ratio indicates the thickness of the graphene sheets. VGNS from processed cheese showed an I_D/I_G ratio of 0.7 and an I_{2D}/I_G ratio of 1.2, whereas the one from cream cheese had an I_D/I_G ratio of 1.4 and an I_{2D}/I_G peak ratio of 0.95. The thickness of VGNS can also be deduced from high-resolution SEM (Figure S2, Supporting Information) and Raman features. According to the Raman features, the I_{2D}/I_G ratios suggest that our VGNS derived from cheese consists of few-layered graphene sheets

DOI: 10.1021/sc500806s
ACS Sustainable Chem. Eng. 2015, 3, 544−551

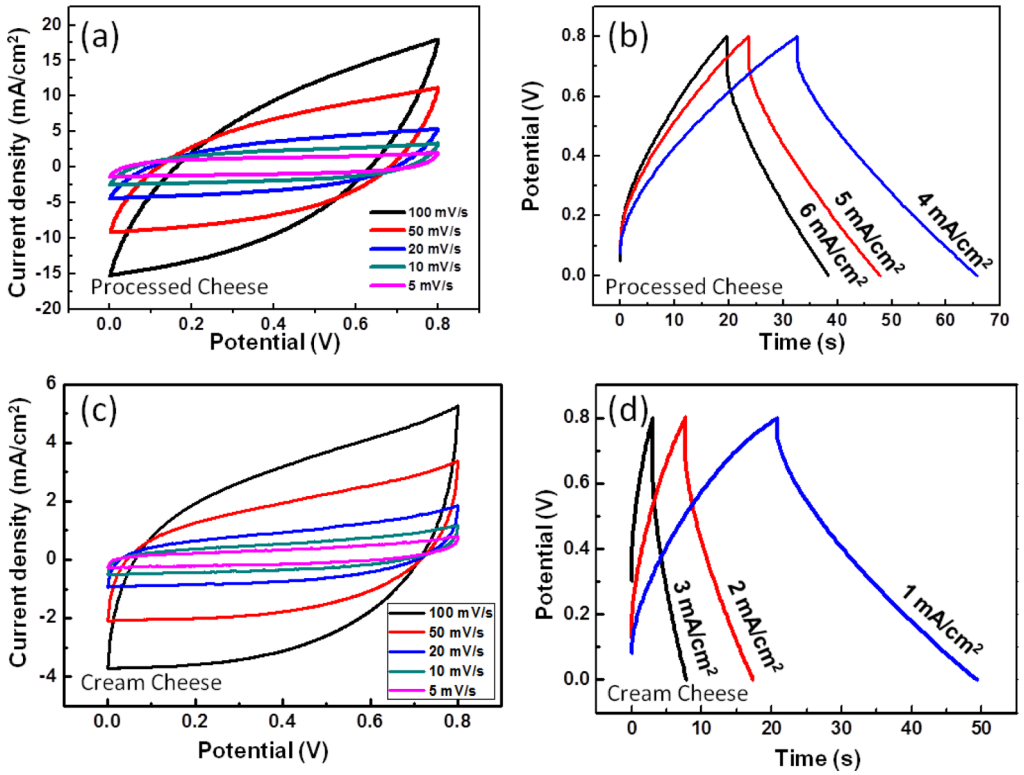

Figure 3. Electrochemical activity of the high mass loading VGNS as obtained from processed and cream cheeses in the two-electrode configuration. Cyclic voltammetry (CV) curves of both processed and cream cheeses at various scan rates are plotted in panels (a) and (c) respectively. Similarly, Galvanostatic charge/discharge curves are plotted in panels (b) and (d).

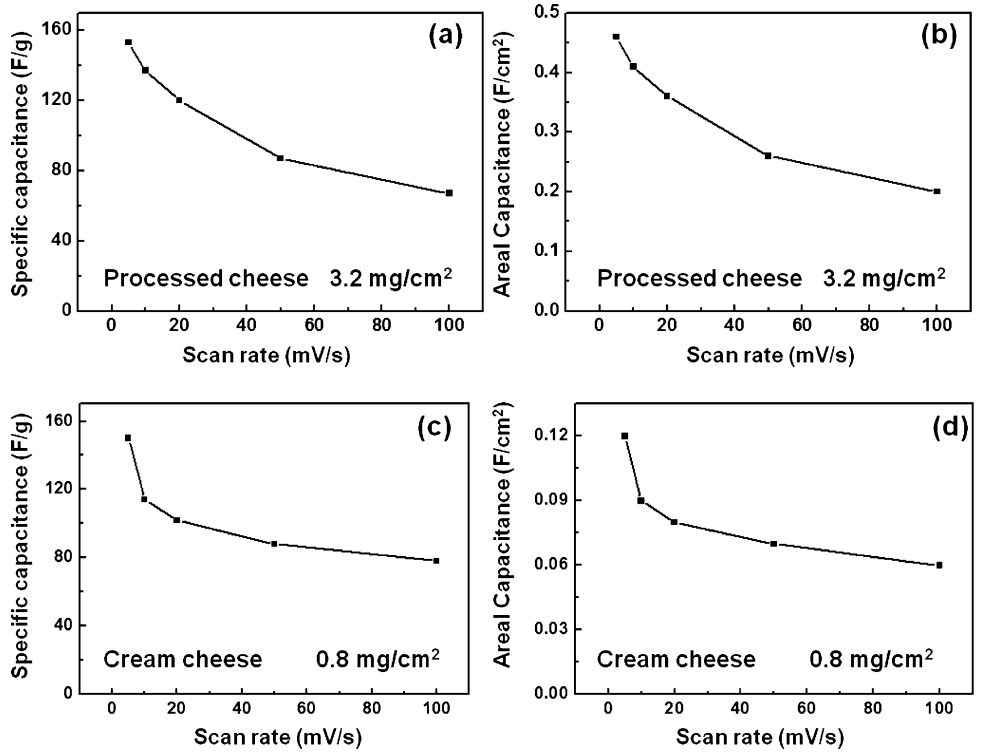

Figure 4. Specific capacitance (a, c) and areal capacitance (b, d) at different scan rates of the high mass loading VGNS electrodes derived from processed and cream cheeses.

(bi- to tri-layer in the edge planes with a thicker basal plane).[34,35] Moreover, the high transparency of VGNS as shown in the SEM image is usually observed for few-layered graphenes (Figure S2, Supporting Information).[36,37] These results thus demonstrate the formation of high-quality VGNS from cheese precursors.

DOI: 10.1021/sc500806s
ACS Sustainable Chem. Eng. 2015, 3, 544−551

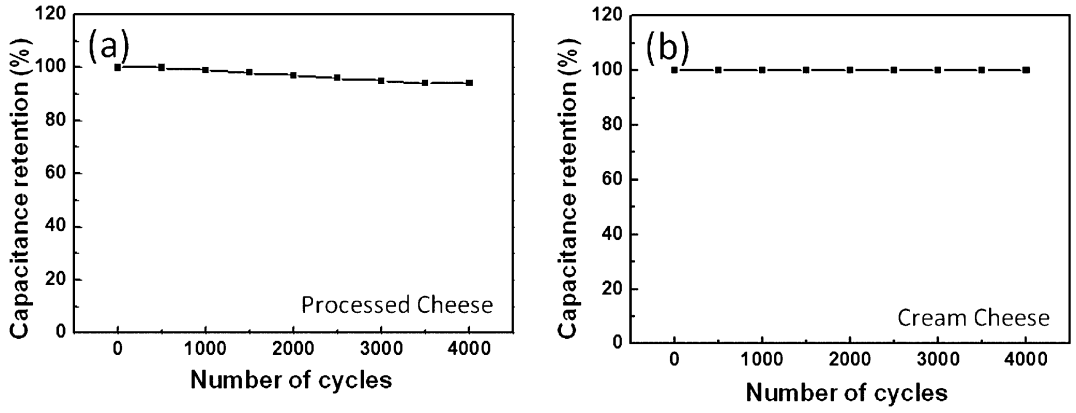

Figure 5. Cycle stability of the high mass loading VGNS electrodes derived from processed (a) and cream (b) cheese precursors for 4,000 cycles at a scan rate of 400 mV/s.

Panels (c) and (f) of Figure 2 illustrate the XPS measurements of VGNS derived from processed and cream cheeses, respectively. In both spectra, a strong C 1s peak positioned at the binding energy (BE) of about 284.5 eV was observed, together with a small amount of oxygen at the BE of 532 eV.[38] This indicates that the cheese-derived structures were predominantly composed of carbon atoms with a small amount of oxygen. Chemical composition analysis of VGNS derived from processed and cream cheeses revealed C atoms at 98.4 and 95.3 atom % and O atoms at 1.6 and 4.7 atom %, respectively. Panels (a) and (b) of Figure S3 of the Supporting Information show the C 1s narrow scans of VGNS derived from processed and cream cheeses, respectively. Both C 1s spectra can be deconvoluted into three distinct peaks corresponding to the C−C (BE ∼ 284.5 eV), oxygenated carbon (BE ∼ 285.4 eV), and shakeup energy-loss feature (BE ∼ 290.2 eV).[24,39,40] Importantly, all VGNS samples featured a high fraction of sp^2-hybridized carbon, suggesting the high quality of the graphene sheets. To demonstrate the specific surface area and materials texture of the VGNS electrodes, BET measurements were also performed. The results revealed a surface area of 448 m^2/g with a typical mesoporous structure (Figure S4, Supporting Information). Consequently, this favorable morphology is expected to facilitate the adsorption of ions for the EDL formation and enable the cheese-derived VGNS to deliver good electrochemical properties.

The electrochemical performances of VGNS derived from processed and cream cheeses was then investigated by potentiostat/galvanostat with the two- and three-electrode configurations. Panels (a) and (c) of Figure 3 show the cyclic voltammetry (CV) curves of VGNS derived from processed and cream cheeses in 1 M Na_2SO_4 aqueous electrolyte, respectively, measured in the two-electrode configuration. It is noticeable that the CV shapes were rectangular and symmetric at low scan rates (5−20 mV/s), reflecting that both electrodes exhibited an efficient formation of EDL and fast ion transport. Nevertheless, the CV curves became skewed at high scan rates (e.g., >100 mV/s). Panels (b) and (d) of Figure 3 show the galvanostatic charge/discharge curves of VGNS at different current densities from 1 to 6 mA/cm^2. Both cheese-derived VGNS exhibited a linear dependence of charge/discharge potential with time, suggesting the dominance of the EDL mechanism.[41] Correspondingly, the specific capacitance C_s was calculated from the CV curves at different scan rates, as shown in panels (a) and (c) of Figure 4. Both VGNS derived from processed and cream cheeses exhibited a high specific capacitance of 156 and 151 F/g at 5 mV/s, respectively. The values were obtained from the two-electrode measurements as it avoids the possibility of overstating the results that may arise from the three-electrode system. The two-electrode test is more commonly used in real supercapacitor devices.[42] Nevertheless, we have also calculated the specific capacitance from the three-electrode system because it characterizes the full potential of a specific nanomaterial. The results obtained from the three-electrode measurement showed good agreement with the two-electrode measurements (Figure S5, Supporting Information).

Typically, as the mass loading of the electrode material increases, the specific capacitance of the supercapacitor decreases due to the inaccessible surface areas and the impaired ion diffusion. However, this trend was not evident for VGNS obtained by the plasma reforming of cheese precursors in the present case. Despite a significant increase in the mass loading (from 0.8 to 3.2 mg/cm^2), a relatively constant C_s was obtained (from 151 to 156 F/g). As the graphene sheets are vertically oriented with respect to the growth substrate, our VGNS structures maintain the accessible surface area and facilitate the diffusion of ions even at high mass loadings. This unique feature is important for future developments in high-capacity graphene-based supercapacitors. Furthermore, VGNS derived from cream cheese showed a 53% capacitance retention when the scan rate increased from 5 to 100 mV/s (Figure 4c), whereas the one derived from processed cheese also retained 41% (Figure 4a). Such rate capabilities of cheese-derived VGNS remained superior as compared to other graphene-based electrodes. These results suggest that ion accessibility and ion transport are greatly facilitated by the vertical alignment of graphene nanosheets in the electrode materials.

Panels (b) and (d) of Figure 4 show the areal capacitance of VGNS derived from both processed and cream cheeses at different scan rates. In particular, VGNS derived from processed cheese demonstrated a very high areal capacitance of 0.46 F/cm^2 at 5 mV/s, whereas the one from cream cheese also exhibited 0.12 F/cm^2 at the same scan rate. The lower areal capacitance of the latter reflects the lower mass loading in that case. Notably, our results show that a 4-fold increase in mass loading leads to an approximately 4-fold increase in the areal capacitance. This proportional increase in areal capacitance may be attributed to the vertical alignment of graphene sheets. The obtained areal capacitances are among the highest values achieved so far for pure graphene- and carbon-based super-

DOI: 10.1021/sc500806s
ACS Sustainable Chem. Eng. 2015, 3, 544−551

capacitors (Table S1, Supporting Information).[16,18−21,43−46] For instance, Zhou et al. reported a value of 0.152 F/cm^2 for chemically processed graphenes.[19]

The stability tests of VGNS-based electrodes are shown in panels (a) and (b) of Figure 5, where the electrodes were performed for over 4000 cycles at a scan rate of 400 mV/s. Notably, VGNS derived from cream and processed cheeses exhibited the capacity retention of 99% and 94%, respectively. This stability is comparable to the many other graphene- and carbon-based supercapacitors with high mass loadings as reported elsewhere (Table S1, Supporting Information).[20,47−49] For instance, Maiti et al. reported a 97.8% retention after 5000 cycles for graphene-based supercapacitors.[20] Zhang et al. obtained a 98% stability after 1000 cycles for CNT-integrated electrodes,[44] and Puthusseri et al. demonstrated a 90% retention after 5000 cycles with 3D porous carbons.[49]

The electrochemical impedance spectra (EIS) for VGNS obtained from the plasma reforming processes are shown in Figure S6 of the Supporting Information, where the frequency-dependent impedance is plotted as the real (Z′) and imaginary (Z″) components. Both samples displayed a linear line with a high slope at low frequencies, indicating a near-ideal capacitive behavior. The presence of amorphous carbon in the basal plane of VGNS structure may result in the deviation from a vertical line in the spectra. In the high-frequency range, a semi-circle was observed to intersect with the real (Z′) axis in both spectra, which could be attributed to charge transfer at the electrode−electrolyte interface. The equivalent series resistance can be extrapolated from the point of intersection, which was about 4 Ω for both VGNS electrodes. The good conductivity of electrodes can be attributed to the high quality of VGNS and the good binding of VGNS to the growth substrate, as enabled by the single-step plasma transformation process. In addition, we have also performed the three-electrode cell measurements to better evaluate the potential of cheese-derived VGNS electrode materials (Figure S7, Supporting Information). Overall, our VGNS exhibit energy storage capabilities that are among the best for carbon-based devices (Table S1, Supporting Information). While the fabrication of carbon-based electrodes often involves complex and resource-consuming processes, this single-step plasma reforming of cheese precursors is clearly an energy efficient, potentially scalable, and chemically green alternative for the direct assembly of high-performance VGNS-based supercapacitors.

To further understand the effects of precursor composition on the resulting VGNS nanostructure, we also utilized fat-reduced processed cheese as the precursor. Compared to the normal processed cheese, fat-reduced processed cheese typically contains 8−10 wt % water and includes fat substitutes and mimetics as replacers.[50] After the same single-step plasma process, fat-reduced processed cheeses were also transformed into VGNS with a mass loading of 2.8 mg/cm^2. However, the resulting nanostructure contained more defects and thicker graphene sheets, as compared to the VGNS derived from processed cheese precursor (Figure S8, Supporting Information). In addition, the fat-reduced cheese precursor resulted in VGNS with notable deposits of amorphous carbon. From the XPS elemental analysis, VGNS derived from fat-reduced processed cheese were comprised of carbon, oxygen, and potassium at concentrations of 72.9, 15.5, and 11.6 atom % (Figure S8c, Supporting Information). The high K and O contents of the structure were in contrast to the VGNS grown by either processed or cream cheeses. This difference most likely originated from the artificial additives and fat replacers used in the production of fat-reduced cheese. Electrochemically, VGNS derived from fat-reduced cheese exhibited a C_s of 153 F/g at 5 mV/s and an areal capacitance of 0.38 F/cm^2, similar to those obtained from processed cheese precursors. However, only 34% capacitance retention was observed when the scan rate was increased from 5 to 100 mV/s. This was significantly lower than those obtained from the processed and cream cheese precursors. Moreover, nonideal capacitor behavior was observed, as evidenced by the skewed charge/discharge curves (Figure S8g, Supporting Information). The resulting VGNS also demonstrated a higher equivalent series resistance, as compared to VGNS derived from the processed and cream cheeses (Figure S8h, Supporting Information). These results reveal that the presences of artificial additives and fat-replacers in cheese precursor can reduce the graphitic content of VGNS and significantly impede their electrochemical performance. Overall, we have demonstrated a good supercapacitor performance using VGNS-based structures derived from cheese. In addition, as VGNS has a porous structure, it can act as a versatile platform material to accommodate heteronanostructures. Therefore, by decorating these areas of VGNS with other nanostructures that exhibit good electrochemical properties, it may be possible to significantly enhance the performance of VGNS-based supercapacitors due to the as yet unexplored synergistic effects.

We denote that in the conversion of natural precursors using plasmas, the plasma parameters also play a critical role in determining the resulting properties.[51] Therefore, to demonstrate the plasma-related control and understand the temporal dynamics of the transformation of cheese into VGNS, we performed many experiments to find the optimum conditions. Over the course of experiments, the plasma treatment time and hydrogen concentration were found to be critical for the growth of VGNS. When the plasma processing time was prolonged or an excessive hydrogen concentration was used, the presence of graphitic nanostructures dramatically reduced, as evidenced by the microstructural observations and Raman spectra (Figure S9, Supporting Information). Similarly, when the plasma processing time was reduced beyond the threshold or the hydrogen concentration was too low, we observed the transformation process to be incomplete (Figure S9, Supporting Information). Therefore, our experiments show that the transformation of natural precursors into VGNS requires precise control over the plasma processing parameters. This is the key for obtaining good quality graphene sheets with favorable electrochemical properties for energy storage devices.

CONCLUSION

In summary, we have developed a single-step, low-temperature plasma process to produce high-quality VGNS structures with a high mass loading using cheeses as the precursors. Moreover, a direct integration of VGNS with the growth substrates was successfully demonstrated. As a result of the direct integration of high-quality VGNS with high mass loading, one of the highest-to-date areal capacitances (0.46 F/cm^2) of VGNS-based electrodes was achieved. VGNS also exhibited minimum degradation in electrochemical properties despite a significant increase in mass loading of the electrode. Furthermore, we have demonstrated that nonequilibrium low-temperature plasmas are effective and versatile nanofabrication tools that break down and rebuild diverse forms of precursors of different chemical compositions and states of matter into functional VGNS

DOI: 10.1021/sc500806s
ACS Sustainable Chem. Eng. 2015, 3, 544−551

structures. These results thus provide a critical step in the development of graphene-based, high-performance energy storage devices.

■ ASSOCIATED CONTENT

Supporting Information

Photographic and SEM images of the cheese precursors and VGNS electrodes derived from plasma, deconvoluted C 1s peaks of processed and cream cheeses, BET measurement, EIS spectra, cyclic voltammetry and galvanostatic charge−discharge curves obtained from the three-electrode setup, VGNS derived from fat-reduced processed cheese and its electrochemical performance, results of nonoptimal growth conditions, and comparison of supercapacitor performance of graphene- and carbon-based nanostructures with high mass loadings. This material is available free of charge via the Internet at http://pubs.acs.org.

■ AUTHOR INFORMATION

Corresponding Author

*Fax: (+61) 02 9413 7200. E-mail: Kostya.ostrikov@csiro.au.

Author Contributions

Dong Han Seo and Samuel Yick contributed equally.

Notes

The authors declare no competing financial interest.

■ ACKNOWLEDGMENTS

This work is supported by the Australian Research Council (ARC) and CSIRO's OCE Science Leadership Program. D.H.S. acknowledges the CSIRO OCE Postdoctoral Fellowship Program. S.P. acknowledges APA and the CSIRO's OCE top-up scholarship. Z.J.H. and K.O. acknowledge DECRA and the Future Fellowships from the ARC, respectively.

■ REFERENCES

(1) Tollefson, J. How green is my future? *Nature* **2011**, *473* (7346), 134−135.

(2) Service, R. F. New 'supercapacitor' promises to pack more electrical punch. *Science* **2006**, *313* (5789), 902.

(3) Manthiram, A.; Fu, Y.; Su, Y.-S. In charge of the world: Electrochemical energy storage. *J. Phys. Chem. Lett.* **2013**, *4* (8), 1295−1297.

(4) Yang, Z.; Zhang, J.; Kintner-Meyer, M. C. W.; Lu, X.; Choi, D.; Lemmon, J. P.; Liu, J. Electrochemical energy storage for green grid. *Chem. Rev.* **2011**, *111* (5), 3577−3613.

(5) Miller, J. R.; Simon, P. Electrochemical capacitors for energy management. *Science* **2008**, *321* (5889), 651−652.

(6) Li, X.; Wei, B. Supercapacitors based on nanostructured carbon. *Nano Energy* **2013**, *2* (2), 159−173.

(7) Simon, P.; Gogotsi, Y. Capacitive energy storage in nanostructured carbon−electrolyte systems. *Acc. Chem. Res.* **2013**, *46* (5), 1094−1103.

(8) Staaf, L. G. H.; Lundgren, P.; Enoksson, P. Present and future supercapacitor carbon electrode materials for improved energy storage used in intelligent wireless sensor systems. *Nano Energy* **2014**, *9* (0), 128−141.

(9) Wu, Z.-K.; Lin, Z.; Li, L.; Song, B.; Moon, K.-s.; Bai, S.-L.; Wong, C.-P. Flexible micro-supercapacitor based on in-situ assembled graphene on metal template at room temperature. *Nano Energy* **2014**, *10* (0), 222−228.

(10) Miller, J. R.; Outlaw, R. A.; Holloway, B. C. Graphene double-layer capacitor with ac line-filtering performance. *Science* **2010**, *329* (5999), 1637−1639.

(11) Yang, P.; Mai, W. Flexible solid-state electrochemical supercapacitors. *Nano Energy* **2014**, *8* (0), 274−290.

(12) El-Kady, M. F.; Strong, V.; Dubin, S.; Kaner, R. B. Laser scribing of high-performance and flexible graphene-based electrochemical capacitors. *Science* **2012**, *335* (6074), 1326−1330.

(13) Yang, X.; Zhu, J.; Qiu, L.; Li, D. Bioinspired effective prevention of restacking in multilayered graphene films: Towards the next generation of high-performance supercapacitors. *Adv. Mater.* **2011**, *23* (25), 2833−2838.

(14) Cheng, Y.; Lu, S.; Zhang, H.; Varanasi, C. V.; Liu, J. Synergistic effects from graphene and carbon nanotubes enable flexible and robust electrodes for high-performance supercapacitors. *Nano Lett.* **2012**, *12* (8), 4206−4211.

(15) Sheng, K.; Sun, Y.; Li, C.; Yuan, W.; Shi, G. Ultrahigh-rate supercapacitors based on eletrochemically reduced graphene oxide for ac line-filtering. *Sci. Rep.* **2012**, *2*, 247.

(16) Cai, M.; Outlaw, R. A.; Quinlan, R. A.; Premathilake, D.; Butler, S. M.; Miller, J. R. Fast response, vertically oriented graphene nanosheet electric double layer capacitors synthesized from C_2H_2. *ACS Nano* **2014**, *8* (6), 5873−5882.

(17) Gogotsi, Y.; Simon, P. True performance metrics in electrochemical energy storage. *Science* **2011**, *334* (6058), 917−918.

(18) Yoon, Y.; Lee, K.; Kwon, S.; Seo, S.; Yoo, H.; Kim, S.; Shin, Y.; Park, Y.; Kim, D.; Choi, J.-Y.; Lee, H. Vertical alignments of graphene sheets spatially and densely piled for fast ion diffusion in compact supercapacitors. *ACS Nano* **2014**, *8* (5), 4580−4590.

(19) Zhou, H. H.; Han, G. Y.; Xiao, Y. M.; Chang, Y. Z.; Zhai, H. J. Facile preparation of polypyrrole/graphene oxide nanocomposites with large areal capacitance using electrochemical codeposition for supercapacitors. *J. Power Sources* **2014**, *263*, 259−267.

(20) Maiti, U. N.; Lim, J.; Lee, K. E.; Lee, W. J.; Kim, S. O. Three-dimensional shape engineered, interfacial gelation of reduced graphene oxide for high rate, large capacity supercapacitors. *Adv. Mater.* **2014**, *26* (4), 615−619.

(21) Hahm, M. G.; Leela Mohana Reddy, A.; Cole, D. P.; Rivera, M.; Vento, J. A.; Nam, J.; Jung, H. Y.; Kim, Y. L.; Narayanan, N. T.; Hashim, D. P.; Galande, C.; Jung, Y. J.; Bundy, M.; Karna, S.; Ajayan, P. M.; Vajtai, R. Carbon nanotube−nanocup hybrid structures for high power supercapacitor applications. *Nano Lett.* **2012**, *12* (11), 5616−5621.

(22) Dyatkin, B.; Presser, V.; Heon, M.; Lukatskaya, M. R.; Beidaghi, M.; Gogotsi, Y. Development of a green supercapacitor composed entirely of environmentally friendly materials. *ChemSusChem* **2013**, *6* (12), 2269−2280.

(23) Green Chemistry's 12 Principles. U.S. Environmental Protection Agency. http://www2.epa.gov/green-chemistry/basics-green-chemistry#twelve (accessed January 2015).

(24) Seo, D. H.; Han, Z. J.; Kumar, S.; Ostrikov, K. Structure-controlled, vertical graphene-based, binder-free electrodes from plasma-reformed butter enhance supercapacitor performance. *Adv. Energy Mater.* **2013**, *3* (10), 1316−1323.

(25) Seo, D. H.; Rider, A. E.; Han, Z. J.; Kumar, S.; Ostrikov, K. Plasma break-down and re-build: Same functional vertical graphenes from diverse natural precursors. *Adv. Mater.* **2013**, *25* (39), 5638−5642.

(26) Seo, D. H.; Yick, S.; Han, Z. J.; Fang, J. H.; Ostrikov, K. Synergistic fusion of vertical graphene nanosheets and carbon nanotubes for high-performance supercapacitor electrodes. *ChemSusChem* **2014**, *7* (8), 2317−2324.

(27) Kapoor, R.; Metzger, L. E. Process cheese: Scientific and technological aspects—A review. *Compr. Rev. Food Sci. Food Saf.* **2008**, *7* (2), 194−214.

(28) Bradley, R. L. V.; Margaret, A. Determination of moisture in cheese and cheese products. *J. AOAC Int.* **2001**, *84* (2), 570−592.

(29) Brighenti, M.; Govindasamy-Lucey, S.; Lim, K.; Nelson, K.; Lucey, J. A. Characterization of the rheological, textural, and sensory properties of samples of commercial US cream cheese with different fat contents. *J. Dairy Sci.* **2008**, *91* (12), 4501−4517.

(30) Lespade, P.; Al-Jishi, R.; Dresselhaus, M. S. Model for Raman scattering from graphitized carbons. *Carbon* **1982**, *20*, 427.

DOI: 10.1021/sc500806s
ACS Sustainable Chem. Eng. 2015, 3, 544−551

(31) Wang, Y.; Alsmeyer, D. C.; McCreery, R. L. Raman spectroscopy of carbon materials: Structural basis of observed spectra. *Chem. Mater.* **1990**, *2*, 557.
(32) Cuesta, A.; Dhamelincourt, P.; Laureyns, J.; Martinez-Alonso, A.; Tascon, J. M. D. Comparative performance of X-ray diffraction and Raman microprobe techniques for the study of carbon materials. *J. Mater. Chem.* **1998**, *8*, 2875.
(33) Niyogi, S.; Bekyarova, E.; Itkis, M. E.; Zhang, H.; Shepperd, K.; Hicks, J.; Sprinkle, M.; Berger, C.; Lau, C. N.; de Heer, W. A.; Conrad, E. H.; Haddon, R. C. Spectroscopy of covalently functionalized graphene. *Nano Lett.* **2011**, *10*, 4061.
(34) Wu, W.; Yu, Q. K.; Peng, P.; Liu, Z. H.; Bao, J. M.; Pei, S. S. Control of thickness uniformity and grain size in graphene films for transparent conductive electrodes. *Nanotechnology* **2012**, *23* (3), 035603.
(35) Seo, D. H.; Kumar, S.; Ostrikov, K. Thinning vertical graphenes, tuning electrical response: From semiconducting to metallic. *J. Mater. Chem.* **2011**, *21* (41), 16339−16343.
(36) Kim, D.; Han, J. Y.; Lee, D.; Lee, Y.; Jeon, D. Y. Facile conversion of a cellulose acetate laminate film to graphene by a lamination process and post-annealing. *J. Mater. Chem.* **2012**, *22* (37), 20026−20031.
(37) Park, M. H.; Kim, T. H.; Yang, C. W. Thickness contrast of few-layered graphene in SEM. *Surf. Interface Anal.* **2012**, *44* (11−12), 1538−1541.
(38) Datsyuk, V.; Kalyva, M.; Papagelis, K.; Parthenios, J.; Tasis, D.; Siokou, A.; Kallitsis, I.; Galiotis, C. Chemical oxidation of multiwalled carbon nanotubes. *Carbon* **2008**, *46* (6), 833−840.
(39) Yick, S.; Han, Z. J.; Ostrikov, K. Atmospheric microplasma-functionalized 3D microfluidic strips within dense carbon nanotube arrays confine Au nanodots for SERS sensing. *Chem. Commun.* **2013**, *49* (28), 2861−2863.
(40) Wang, X.; Xia, T.; Ntim, S. A.; Ji, Z.; George, S.; Meng, H.; Zhang, H.; Castranova, V.; Mitra, S.; Nel, A. E. Quantitative techniques for assessing and controlling the dispersion and biological effects of multiwalled carbon nanotubes in mammalian tissue culture cells. *ACS Nano* **2010**, *4* (12), 7241−52.
(41) Taberna, P. L.; Simon, P.; Fauvarque, J. F. Electrochemical characteristics and impedance spectroscopy studies of carbon-carbon supercapacitors. *J. Electrochem. Soc.* **2003**, *150* (3), A292−A300.
(42) Stoller, M. D.; Ruoff, R. S. Best practice methods for determining an electrode material's performance for ultracapacitors. *Energy Environ. Sci.* **2010**, *3* (9), 1294−1301.
(43) Chen, T.; Xue, Y. H.; Roy, A. K.; Dai, L. M. Transparent and stretchable high-performance supercapacitors based on wrinkled graphene electrodes. *ACS Nano* **2014**, *8* (1), 1039−1046.
(44) Zhang, D. H.; Miao, M. H.; Niu, H. T.; Wei, Z. X. Core-spun carbon nanotube yarn supercapacitors for wearable electronic textiles. *ACS Nano* **2014**, *8* (5), 4571−4579.
(45) Bai, Y.; Du, M.; Chang, J.; Sun, J.; Gao, L. Supercapacitors with high capacitance based on reduced graphene oxide/carbon nanotubes/NiO composite electrodes. *J. Mater. Chem. A* **2014**, *2* (11), 3834−3840.
(46) Yu, D. S.; Goh, K.; Wang, H.; Wei, L.; Jiang, W. C.; Zhang, Q.; Dai, L. M.; Chen, Y. Scalable synthesis of hierarchically structured carbon nanotube-graphene fibres for capacitive energy storage. *Nat. Nanotechnol* **2014**, *9* (7), 555−562.
(47) Salunkhe, R. R.; Hsu, S. H.; Wu, K. C. W.; Yamauchi, Y. Large-scale synthesis of reduced graphene oxides with uniformly coated polyaniline for supercapacitor applications. *ChemSusChem* **2014**, *7* (6), 1551−1556.
(48) Peng, C. X.; Wen, Z. B.; Qin, Y.; Schmidt-Mende, L.; Li, C. Z.; Yang, S. H.; Shi, D. L.; Yang, J. H. Three-dimensional graphitized carbon nanovesicles for high- performance supercapacitors based on ionic liquids. *ChemSusChem* **2014**, *7* (3), 777−784.
(49) Puthusseri, D.; Aravindan, V.; Madhavi, S.; Ogale, S. 3D micro-porous conducting carbon beehive by single step polymer carbonization for high performance supercapacitors: The magic of in situ porogen formation. *Energy Environ. Sci.* **2014**, *7* (2), 728−735.
(50) Johnson, M. E.; Kapoor, R.; McMahon, D. J.; McCoy, D. R.; Narasimmon, R. G. Reduction of sodium and fat levels in natural and processed cheeses: Scientific and technological aspects. *Compr. Rev. Food Sci. Food Saf.* **2009**, *8* (3), 252−268.
(51) Ostrikov, K.; Neyts, E. C.; Meyyappan, M. Plasma nanoscience: From nano-solids in plasmas to nano-plasmas in solids. *Adv. Phys.* **2013**, *62* (2), 113−224.

DOI: 10.1021/sc500806s
ACS Sustainable Chem. Eng. 2015, 3, 544−551